

# Multiheterodyne Characterization of Excess Phase Noise in Atmospheric Transfer of a Femtosecond-Laser Frequency Comb

Ravi P. Gollapalli, *Student Member, IEEE, OSA*, and Lingze Duan, *Member, IEEE, OSA*

**Abstract**—We report an experimental investigation on remote transfer of a femtosecond-laser frequency comb through an open atmospheric link. Optical multiheterodyne is used to measure the excess phase noise and the frequency stability of the transferred comb. The dispersion of air is found to have a minimal impact on the multiheterodyne signal, and the effectiveness of the technique to characterize the behaviors of comb lines under the influence of turbulence is theoretically analyzed. Large phase modulation due to the index fluctuation of the air over a 60-m transmission link is found to cause a significant linewidth broadening. Under low-wind conditions, a fractional frequency stability in the order of  $10^{-14}$  has been achieved over several minutes with a 1-s averaging time. A comparison of this work with previous tests based on continuous wave (CW) lasers indicates that pulsed lasers can work as well as CW lasers for remote transfer of optical frequency references through the atmosphere.

**Index Terms**—Atmospheric transmission, frequency comb, multiheterodyne, phase noise, ultrafast optics.

## I. INTRODUCTION

REMOTE transfer of optical reference frequencies has attracted considerable research interest in recent years due to the increasing need for ultrahigh-precision timing synchronization in fundamental physics, large-scale precision instrumentation, navigation, and communications [1]–[9]. Conventionally, optical frequency transfer is accomplished by sending a highly stable optical carrier from a continuous wave (CW) laser across a fiber link [1]–[3]. A drawback of this scheme is that it relies on the availability of a fiber-optic link, which, in many cases, leads to higher overall cost and a lack of flexibility. In addition, future timing references are likely space borne [6], making any wired synchronization schemes impractical. Recently, the concept of free-space optical timing distribution has been proposed to address the aforementioned challenges [7]–[9]. Coherent transfer of single-frequency

optical carriers has been demonstrated, first over a 100-m rooftop link using a CW diode laser [8], and then across a 5-km ground–ground link using a Nd:YAG laser [9].

An important limitation of these CW laser-based transfer schemes is that each laser can only deliver one reference frequency. When the clocks on the remote sites operate at different optical frequencies or at radio frequencies (RF), a flywheel system such as an optical frequency comb has to be used to bridge the frequency gaps. Such a requirement increases the system complexity for the users and may restrict the applications of these schemes. Recently, pulsed lasers have emerged as an alternative means to disseminate optical reference frequencies. By directly broadcasting a femtosecond-laser (FL) frequency comb through a transmission network, one can simultaneously deliver a large number (e.g.,  $\sim 10^5$ ) of frequency references spanning across a broad spectrum to remote users and allow them to conveniently synchronize clocks running at different frequencies (in both optical and RF ranges) to the reference laser [4]–[6]. Optical-frequency transfer based on a mode-locked laser has been shown to have comparable reliability to CW laser-based transfer in optical fibers [4], and FLs have been used to achieve highly stable optical–optical synchronization between lasers through a fiber link [5]. However, there has been no report addressing the important method of free-space optical frequency distribution with FL frequency combs. A demonstration of such a scheme is necessary, because some of the unique factors associated with turbulent atmospheres and phase-noise characterization of pulses are drastically different from the cases involving fiber-optic transmission or CW lasers and, therefore, deserve some in-depth investigation.

In this paper, we report an experimental demonstration of optical-frequency transfer through open atmospheres based on an FL frequency comb. The goal is to characterize the excess phase noise and the optical-frequency instability induced by the atmospheric transmission. Note that this work must be distinguished from some of the previous reports on the atmospheric transfer of RF timing references using a frequency comb [7], [10]. In Sections II and IV, we will describe our experimental setup and measurement results, respectively. A unique technique used in our noise characterization is optical multiheterodyne. Despite the growing use of multiheterodyne in recent years for various applications of frequency combs [11], [12], its effectiveness in phase-noise characterization has not been analyzed to the best of our knowledge. In Section III, we will address this question

Manuscript received July 01, 2011; revised September 07, 2011; accepted September 15, 2011. Date of publication September 26, 2011; date of current version November 09, 2011.

R. P. Gollapalli was with the University of Alabama in Huntsville, Huntsville, AL 35899 USA. He is now with the Department of Electrical and Computer Engineering, University of South Alabama, Mobile, AL 36688 USA (e-mail: gollapalli@jaguar1.usouthal.edu).

L. Duan is with the Department of Physics, the University of Alabama in Huntsville, Huntsville, AL 35899 USA (e-mail: lingze.duan@uah.edu).

Color versions of one or more of the figures in this paper are available online at <http://ieeexplore.ieee.org>.

Digital Object Identifier 10.1109/JLT.2011.2169449

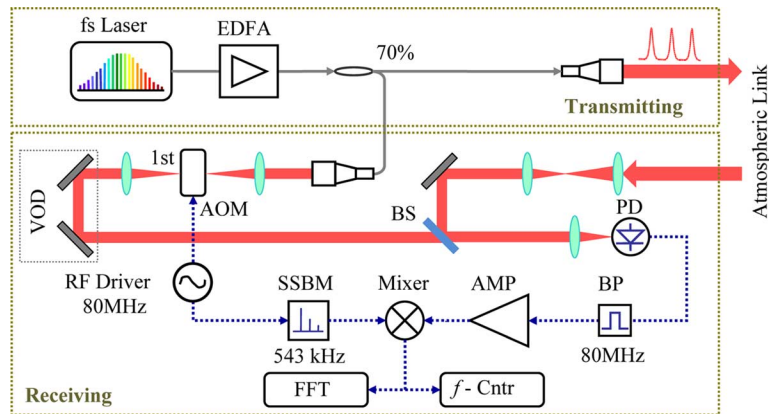


Fig. 1. Schematic layout of the experimental system for atmospheric transfer of optical frequency references using an FL frequency comb. AMP: microwave amplifiers; AOM: acousto-optic modulator; BS: beam splitter; EDFA: erbium-doped fiber amplifier; FFT analyzer: fast Fourier transform analyzer; PD: photodiode; SSBM: single-sideband modulator; and VOD: variable optical delay.

in the context of femtosecond pulses propagating through a turbulent and dispersive atmospheric path. Finally, in Section V, we will compare our experimental results with previous reports on atmospheric transfer of optical frequency references using CW lasers and then summarize.

## II. EXPERIMENTAL SETUP

The atmospheric laser transmission link is set up on the roof of our laboratory building on the campus of the University of Alabama in Huntsville, Huntsville, AL. A sturdy steel tripod anchored on the rooftop platform houses a 2-in gold mirror, which serves as the beam reflector. The laser beam is launched from an astronomical observatory into the open air and the reflector sends the beam back to the observatory, where all the signal processing and measurement takes place. The round-trip propagation distance is about 60 m. The entire transmission link is about 20 m above the ground and has no high-rise buildings nearby to alter the wind patterns.

Fig. 1 shows a schematic layout of the experimental setup. The system is divided into transmitting and receiving subsystems. In the transmitting subsystem, a commercial fiber laser (Precision Photonics FFL-1560) generates a train of 150-fs pulses at a repetition rate of 90 MHz. An erbium-doped fiber amplifier (EDFA) boosts the average power to 100 mW. The optical spectrum at the output of the EDFA has a 3-dB bandwidth of 40 nm centered at 1562 nm. A broadband fiber coupler directs 70% of the optical power to a fiber collimator, where a laser beam of 7-mm diameter is launched into the atmospheric transmission link. The remaining laser power ( $\sim 30\%$ ) is collimated by a second fiber collimator and used as the reference beam. In the receiving subsystem, the reference beam passes through an acousto-optic modulator (AOM), which is driven by an RF driver at 80 MHz, and the first-order deflection is selected. Meanwhile, the beam transmitted through the atmospheric link is coupled into the receiving subsystem by a lens pair, which converts the expanded beam into a comparable size to the reference beam. The two beams are then combined into collinear propagation at a broadband beam splitter and focused onto a photodiode. A variable optical delay line in the reference

arm ensures temporal overlapping of the transmitted pulses and the reference pulses. The interference of the two beams on the photodiode produces an 80-MHz beat note, which, upon filtering and amplification, is phase-compared with a portion of the original 80-MHz driving signal at a double-balanced mixer. In order to measure the linewidth of the beat note, a small frequency shift (about 543 kHz) is added to the original 80-MHz signal through a single-sideband modulator (SSBM). The resulted 543-kHz beat signal is analyzed by a fast Fourier transform (FFT) analyzer for direct spectral width measurement and a frequency counter for frequency stability measurement.

Beam wander and speckle are two important atmospheric optical effects that can cause signal amplitude fluctuation [13], which is indistinguishable from phase noise in our experiment. In order to suppress such transmission-induced amplitude noise, we increase the effective aperture of the receiving subsystem by using large-diameter optics and focusing the beam directly onto the photodiode with the size of the focus much smaller than the active area of the detector. A similar receiving system has been used previously in the study of frequency comb-based RF transfer, and has been shown experimentally to be effective in minimizing the impact of beam wander and speckle [10].

## III. MULTIHETERODYNE PHASE-NOISE MEASUREMENT

### A. Multiheterodyne Under the Steady State

Unlike CW lasers, an FL delivers a number of spectral lines simultaneously and can be treated as a free-run frequency comb [14]. In many cases, it is difficult to measure the excess phase noise of each individual spectral line. Instead, the coherent superposition of the phase fluctuation of multiple spectral lines is measured using optical multiheterodyne as described in Section II [4]. In order to understand the principle of this technique in the characterization of excess phase noise, we first consider a simplified version of our experiment in which a long FL pulse train propagates through a highly imbalanced Michelson interferometer in a weakly dispersive medium as shown in Fig. 2(a). The electric field of the pulses can in general be written as  $E(z, t) = A(z, t) \exp(-i\omega_0 t)$ , where  $\omega_0$  is the carrier frequency and  $A(z, t)$  is the periodic function of the

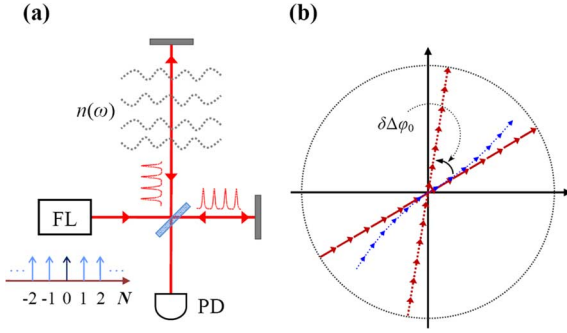


Fig. 2. Principle of multiheterodyne phase-noise measurement. (a) Experimental configuration is simplified to an imbalanced Michelson interferometer, where FL demotes femtosecond laser and PD denotes photodiode. The arm lengths are adjusted so that pulses from both arms arrive to the PD overlapping. The frequency comb generated by the FL is indexed based on the comb line's relation to the carrier (the center frequency in this case). The transmission medium has a dispersion relation characterized by its frequency-dependent index of refraction  $n(\omega)$ . (b) Each of the transmitted comb lines produces a phasor (solid red arrow) by beating with its counterpart from the reference arm. The pulse overlapping condition ensures that all the phasors from individual comb lines superpose in phase to form the multiheterodyne signal, and the correction due to group-delay dispersion is negligible. When  $n(\omega)$  experiences a fluctuation, the dominant effect of the multiheterodyne signal is a rotation of the overall phasor by an amount equal to the phase fluctuation of the carrier  $\delta\Delta\varphi_0$  (dashed red line). The secondary effect is characterized by a distortion of the overall phasor from the straight line (dotted blue line).

pulse envelope.  $A(z, t)$  can be further expanded into a Fourier series [15]

$$A(z, t) = \sum_{N=-\infty}^{\infty} [\tilde{A}(0, \Delta\omega_N) \exp(ik_N z)] \exp(-i\Delta\omega_N t) \quad (1)$$

where  $\Delta\omega_N \equiv 2\pi N f_R$  is the frequency offset of the  $N$ th comb line from the carrier, with  $f_R$  being the pulse repetition rate,  $k_N$  is the propagation constant of the  $N$ th comb line, and  $\tilde{A}(0, \Delta\omega_N)$  is the initial spectral amplitude at  $z = 0$ . The propagation constant relates to the index of refraction of the medium  $n(\omega)$  through the relation  $k_N = n(\omega)\omega/c$ , where  $c$  is the speed of light in vacuum and  $\omega = \omega_0 + \Delta\omega_N$  is the angular frequency of the  $N$ th comb line. For a weakly dispersive medium such as the air, we can expand  $n(\omega)$  at  $\omega_0$  up to the second order to have

$$n(\omega_0 + \Delta\omega_N) \approx n_0 + \frac{dn}{d\omega} \Delta\omega_N + \frac{1}{2} \frac{d^2n}{d\omega^2} (\Delta\omega_N)^2 \quad (2)$$

where  $n_0$  is the index of refraction of the medium at the carrier frequency  $\omega_0$ . This leads to an expansion of the propagation constant  $k_N$

$$k_N(\omega_0 + \Delta\omega_N) = \frac{n_0\omega_0}{c} + \frac{n_g}{c} \Delta\omega_N + \frac{1}{c} \left( \frac{dn}{d\omega} + \frac{\omega_0}{2} \frac{d^2n}{d\omega^2} \right) \Delta\omega_N^2 \quad (3)$$

where  $n_g \equiv n_0 + \omega_0(dn/d\omega)$  is the group index at the carrier frequency. The three terms on the right-hand side of (3) correspond to the carrier phase delay, the group delay, and the group-delay dispersion, respectively.

To perform optical multiheterodyne, the arm lengths of the Michelson interferometer are adjusted so that the return pulses

from the transmission arm overlap with the reference pulses on the photodetector. From a frequency comb point of view, each comb line from the transmission arm beats with its original copy from the reference arm to generate a beat note, which depends on the relative phase delay between the two copies of the comb line. The overall heterodyne signal is the coherent superposition of all these individual beat notes. The relative phase delay for the  $N$ th comb line is  $\Delta\phi_N = k_N \cdot \Delta L$ , where  $\Delta L$  is the path length difference between the two arms of the Michelson interferometer. Due to the pulse-overlapping condition,  $\Delta L$  must satisfy the relation  $\Delta L = Mv_g/f_R$ , where  $M$  is an integer and  $v_g = c/n_g$  is the group velocity of the pulses. These conditions along with (3) lead to an expression for the relative phase delay of the  $N$ th comb line

$$\Delta\phi_N = M \frac{n_0\omega_0}{n_g f_R} + 2MN\pi + \frac{M}{n_g f_R} \left( \frac{dn}{d\omega} + \frac{\omega_0}{2} \frac{d^2n}{d\omega^2} \right) \Delta\omega_N^2. \quad (4)$$

Equation (4) shows that, if the group-delay dispersion of the medium is neglected, the relative phase delays of adjacent comb lines are different by exactly  $2M\pi$ . In multiheterodyne, this means that all the beat notes produced by the individual comb lines superpose in phase on the photodetector, which is illustrated by using a phasor diagram in Fig. 2(b).

This ideal constructive superposition is disrupted by the existence of group-delay dispersion. The extent of the disruption depends on the dispersion of the transmission medium as well as the bandwidth of the heterodyne measurement. To evaluate the impact of dispersion in our experiment, we use the classic dispersion relation for standard air developed by Edlén [16], which we rewrite into a symbolic form of

$$n_s = b_0 + \frac{b_1}{a_1 - \sigma^2} + \frac{b_2}{a_2 - \sigma^2} \quad (5)$$

where  $b_0 = 1 + 8.34213 \times 10^{-5}$ ,  $b_1 = 2.40603 \times 10^{-2} \mu\text{m}^{-2}$ ,  $b_2 = 1.5997 \times 10^{-4} \mu\text{m}^{-2}$ ,  $a_1 = 130 \mu\text{m}^{-2}$ ,  $a_2 = 38.9 \mu\text{m}^{-2}$ , and  $\sigma \equiv 1/\lambda$  is the vacuum wavenumber with the wavelength  $\lambda$  in the unit of micrometer. We also rewrite the third term on the right-hand side of (4) into a form consistent with (5)

$$\Delta\phi_N^{\text{disp}} = 2\pi \frac{MN^2 f_R}{n_{sg} c} \left( \frac{dn_s}{d\sigma} + \frac{\sigma_0}{2} \frac{d^2n_s}{d\sigma^2} \right) \quad (6)$$

where  $\sigma_0$  is the carrier wavenumber in  $\mu\text{m}^{-1}$  and  $n_{sg} \equiv n_s + \sigma(dn_s/d\sigma)$  is the group index for standard air. Combining (5) and (6), we can calculate the dispersion-induced relative phase delay for the comb line immediately next to the carrier, i.e., with  $N = 1$ . The following experimental conditions are used in the calculation:  $f_R = 90$  MHz,  $M = 18$  (according to  $f_R$  and  $\Delta L = 60$  m), and  $\lambda_0 = 1.562 \mu\text{m}$  (the central wavelength of the FL). We also assume  $n_{sg} = 1$  for simplicity. The resulted phase delay is  $\Delta\phi_1^{\text{disp}} = 1.0089 \times 10^{-10}$  rad. For other comb lines, one simply needs to notice that  $\Delta\phi_N^{\text{disp}}$  is proportional to  $N^2$ . For example, in our experiment, the heterodyne bandwidth is limited to about 15 nm (3 dB) around 1562 nm by the transmission band of the AOM. At either edge of this heterodyne band, the absolute value of the comb index is found to be

$|N| \approx 1.025 \times 10^4$ , which leads to a maximum dispersion-induced relative phase delay  $\Delta\phi_{\max}^{\text{disp}} = N^2 \Delta\phi_1^{\text{disp}} = 1.06 \times 10^{-2}$  rad. We therefore reach the conclusion that, under the current experimental conditions, the beat notes produced by individual comb lines superpose onto each other constructively in the multiheterodyne scheme, and the correction to their phases caused by the group-delay dispersion of the air is negligible (much less than  $\pi$ ).

### B. Multiheterodyne With Refractive Index Fluctuations

So far, the discussion is focused on the steady state. When a fluctuation of refractive index occurs in the transmission path, the beat notes of individual comb lines undergo variations of phase and/or amplitude, causing a fluctuation in the overall beat signal on the photodetector. How precisely the fluctuation of this multiheterodyne signal can reflect the excess phase noise acquired by each individual comb line is the key factor determining the accuracy of the multiheterodyne technique. In turbulent atmospheres, the density of air experiences random fluctuations, which leads to fluctuations of refractive index [17]. The index of air under general conditions  $n_{pT}$  can be related to  $n_s$  and thermodynamic state variables by the simple relation of [16]

$$(n_{pT} - 1) = (n_s - 1) \frac{D_{pT}}{D_s} \quad (7)$$

where  $D_{pT}$  is called the density factor, which is a function of pressure  $p$  and temperature  $T$ , and  $D_s$  is the density factor for standard air with a value of 720.775 [16]. The exact form of  $D_{pT}$  is not essential for the current discussion. Interested readers should be able to find more details in [16]. The important message at present, according to (7), is that the dispersion relation of air is independent of density. If we use  $\delta$  to denote the variations induced by air density changes, based on (7), we can easily obtain

$$\delta n_{pT} = (n_{pT} - 1) \frac{\delta D_{pT}}{D_{pT}}. \quad (8)$$

Similarly, we can relate the relative phase delay fluctuation of the  $N$ th comb line to the turbulence-induced index change by

$$\frac{\delta \Delta\phi_N}{\Delta\phi_N} = \frac{\delta n_{pT}}{n_{pT}}. \quad (9)$$

Combining (8), (9), and (4), we obtain a general expression for the phase fluctuation of the  $N$ th comb line in turbulent atmospheres

$$\delta \Delta\phi_N = \left\{ \frac{M n_0 \omega_0}{n_g f_R} + 2MN\pi + \frac{M}{n_g f_R} \times \left( \frac{dn}{d\omega} + \frac{\omega_0}{2} \frac{d^2 n}{d\omega^2} \right) \Delta\omega_N^2 \right\} \cdot \left( 1 - \frac{1}{n_0} \right) \frac{\delta D_{pT}}{D_{pT}} \quad (10)$$

where we have used  $n_0$  to replace  $n_{pT}$  in the multiplication term at the end and all the  $n_0$ ,  $n$ , and  $n_g$  in the dispersion relation (between  $\{\}$ ) should be understood as being under general but steady conditions of  $p$  and  $T$  rather than restricted only to the standard air (for which  $p = 1013.25$  mb and  $T = 15^\circ\text{C}$ ) [18].

It is clear from (10) that the density fluctuation due to turbulence causes every term in the dispersion relation of a comb line fluctuate by the same factor of  $(1 - 1/n_0)\delta D_{pT}/D_{pT}$ . The

dominant contribution, however, comes from the zeroth-order term (proportional to  $\omega_0/f_R$ ), which is a constant for all comb lines. This means that all the individual phasors in Fig. 2(b) would have the same angular variation due to the density fluctuation, and the overall phasor would simply rotate by the same angle as all the individual phasors without changing its magnitude. The first-order term, meanwhile, introduces a phase fluctuation proportional to the mode index  $N$ . Under its influence, the comb lines further away from the carrier would experience larger phase variations. Moreover, the deviation of the group delay from  $2MN\pi$  indicates that the pulses would walk off from their ideal overlapping positions. As a result, the magnitudes of the individual phasors may also change. Both of the effects lead to a distortion of the overall phasor from its straight-line state, as illustrated in Fig. 2(b). The ratio between the first-order and the zeroth-order phase fluctuations is approximately  $2N\pi f_R/\omega_0$ , which at its maximum (at the edge of the measurement band when  $N \sim 10^4$ ) is less than  $10^{-2}$ . Therefore, the fluctuation of group delay induces a secondary effect (distortion) on the multiheterodyne signal, which only becomes significant when the air density fluctuation is large. On the other hand, the second-order term due to group-delay dispersion remains small across the entire measurement band, as shown earlier, and, hence, can be neglected. From the aforementioned analysis, we realize that multiheterodyne measurement gives a well-defined characterization of the comb line phase noise when the turbulence-induced density fluctuation remains small so that the distortion of the overall phasor can be considered negligible. Under such a condition, the excess phase noise measured with the multiheterodyne signal represents the zeroth-order transmission-induced phase fluctuation of all the comb lines, which is also the excess phase noise of the carrier.

Such behaviors of the multiheterodyne signal have been observed in our experiment. First, we have opted to take most of our transfer measurement under low-wind conditions with the wind speed generally below 2 m/s to avoid a significant power fluctuation of the beat notes. Second, in monitoring the frequency stability of the multiheterodyne signal, we have observed two distinct types of behaviors. Within shorter periods ( $\sim 10$  min) after the pulse overlapping is optimized, the heterodyne signal randomly fluctuates around the nominal frequency with a very consistent normal distribution. However, over longer periods, some erratic behaviors, such as sudden dips of the frequency, gradually develop. We found that the occurrence of these frequency dips coincides with increasing fluctuations of the beat note power. Therefore, in the Allan deviation measurement (see Section IV), we used the FFT analyzer to monitor the power of the multiheterodyne signal throughout the experiments so that we can maintain the pulse overlapping close to its optimal state.

## IV. EXPERIMENTAL RESULTS

The frequency transfer test was performed over the course of three months in the summer of 2010. Data have been taken under low-wind conditions with the wind speed below 2 m/s. Strong phase fluctuations in the multiheterodyne signal have been observed as pictured in Fig. 3(a) inset. Time-domain phase traces like Fig. 3(a) inset are taken by mixing the 80-MHz beat

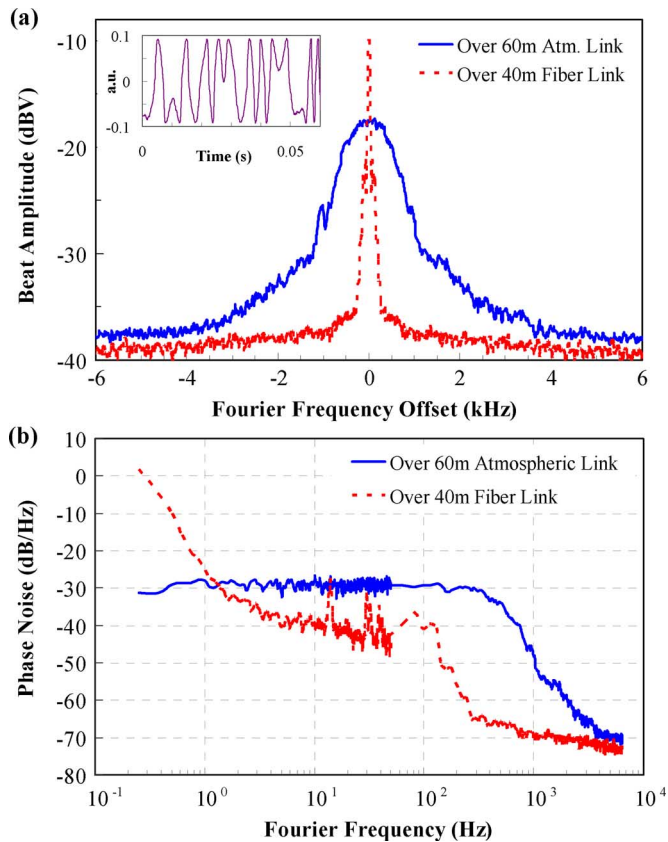


Fig. 3. (a) Fourier spectra of the 543-kHz heterodyne beat note for 60-m atmospheric transfer (solid) and 40-m fiber optic transfer (dashed). Significant linewidth broadening ( $\sim$  kilohertz) is caused by the atmospheric propagation in comparison with fiber transmission. Inset: Time-domain trace of the homodyne beat note for atmospheric transfer demonstrates the large phase fluctuation. (b) Phase-noise spectra of the 543-kHz beat note with the earlier two transfer cases.

note from the photodiode directly with the original 80-MHz AOM driving signal without the SSBM. The fast oscillation of the beat note phase indicates a phase modulation index much greater than  $2\pi$ . In order to examine the Fourier spectrum of the beat note, we add a small frequency offset of 543 kHz using the SSBM onto the 80-MHz reference from the AOM driver so that the beat signals from the mixer are shifted out of the baseband. The resulted beat note spectrum is shown in Fig. 3(a), plotted against the offset frequency from 543 kHz. Also plotted in Fig. 3(a) is the same beat signal without atmospheric transmission, realized by diverting the pulse train in the transmission arm through a fiber link of about 40 m long. The fiber is cut in such a way that it produces the same amount of time delay as the 60-m atmospheric link. Such an arrangement allows us to assess the contribution of the laser and the amplifier in our phase-noise measurement. Due to the imbalance of the interferometer, amplitude and phase noise from the FL and the EDFA could enter the multiheterodyne signal. One particular concern is that, because of the free-running FL, the drift of the laser repetition rate and carrier-envelope offset frequency may also broaden the beat note. With the fiber link, transmission-induced excess phase noise is much smaller [4], allowing us to assess the upper limit of the noise contribution from the laser and the amplifier. In Fig. 3(a), both traces have a resolution bandwidth of 16 Hz, and are averaged over 1 s. The resolu-

tion-limited sharp peak in the spectrum from fiber transmission indicates that the FL and the EDFA have a negligible effect in the current excess phase-noise characterization. In comparison, the atmospheric transmission causes significant spectral broadening. The broadened beat note spectrum has a full width of approximately 1 kHz.

A close look at the noise characteristics of the two transmission cases near the nominal frequency can be gained through their phase-noise spectra, which are assembled from data over two frequency spans and are shown in Fig. 3(b). As discussed in Section III, such multiheterodyne phase noise can be understood as the zeroth-order excess phase noise of all the comb lines, which is also the excess phase noise at the center frequency, in this case, 1562 nm. Since the beat note from the atmospheric transmission has no coherent spike for the carrier, the two curves in Fig. 3(b) are normalized to their total signal powers (i.e., the integration of the beat note spectra) instead of the carrier power. A frequency-independent noise spectrum is seen below 300 Hz for the beat note from the atmospheric transmission. It is followed by a quick roll-off above 500 Hz. Such characteristics seem to agree with the spectral features for a slow phase modulation with a very large modulation index. In comparison, transmission in fiber with the same time delay results in a much smaller phase noise. A similar rolling-off behavior is seen at a much lower frequency ( $\sim$ 100 Hz). Between 1 and 100 Hz, the phase noise shows a  $1/f$  general trend, which indicates a flicker phase noise that is likely caused by the RF amplifiers in the detection subsystem [19]. The spikes in this frequency region are believed to be the result of acoustic noise and electronic interference from the power circuits inside the lab. The aforementioned comparison shows that atmospheric fluctuations add a significant amount of phase noise to the optical frequency references transmitted through the air. As a result, atmospheric transfer of optical frequencies in general suffers much larger short-term fluctuations when compared with fiber-optic transfer.

For many applications, however, a more relevant parameter is the long-term stability of the frequency transfer scheme, which can be evaluated by measuring the Allan deviation of the 543-kHz beat note. Shown in Fig. 4(a) are several sets of measured data of the Allan deviation versus the averaging time through the 60-m transmission link under various weather conditions. Among them, three sets were taken under low-wind conditions, with the wind speed generally staying below 5 mph (miles-per-hour), or 2.2 m/s, throughout the data collection periods (except for Set #1 at 200 s, which is not included here). The average of these data shows an overall behavior of the Allan deviation close to  $1/\tau$  within the measurement range. The fractional frequency stability at 1 s is about  $2 \times 10^{-14}$ . When averaged over 100 s, the stability improves to  $10^{-16}$  level. Over even longer time, however, the beat note often develops large power fluctuation, which prevents a reliable measurement of the Allan deviation with an averaging time longer than 200 s. The fluctuation of the beat note power is believed to be caused by the transmitted and the reference pulses drifting away from their optimum overlapping position due to the change of the effective path length of the transmission link. To demonstrate the effect of wind, we also include here a set of data taken under stronger wind, with wind speed ranging between 7–14

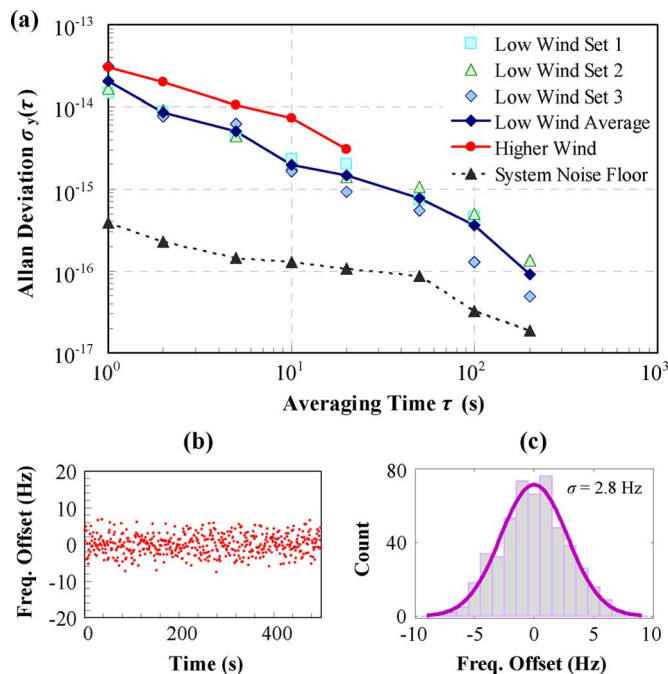


Fig. 4. (a) Allan deviations of the 543-kHz multiheterodyne beat note for 60-m atmospheric transfer under various weather conditions and the system noise floor. (b) Dataset of 500 consecutive frequency measurements at 1-s gate time, plotted relative to the nominal frequency. (c) Histogram of (b), overlaid with a fitting to the normal distribution, leads to a standard deviation of 2.8 Hz for the frequency references transferred across the atmospheric link.

mph over the data collection period. Below 20 s, the higher wind data stay roughly 3 dB above the average low-wind data and display a similar  $1/\tau$  dependence. No Allan deviation was successfully measured above 20 s due to the power fluctuation of the beat note. In addition, a set of baseline data are also included in Fig. 4(a) to mark the system-limited measurement resolution. It is obtained by reflecting the transmission beam immediately into the receiving subsystem, so the length of atmospheric propagation is negligible.

To further verify the scale of the frequency fluctuation, we take a close look at the measured beat note frequencies. Fig. 4(b) shows consecutive readings of the frequency counter over several minutes with a 1-s gate time, taken under the low-wind condition. The frequencies have been offset to the nominal value of 543 kHz. A histogram analysis shows that the frequencies have a normal distribution around the nominal frequency, as shown in Fig. 4(c), and a Gaussian fitting results in a standard deviation of 2.8 Hz. This frequency fluctuation level is in agreement with the Allan deviation measurement for low wind.

## V. DISCUSSION

To put our work into context, it is interesting to compare the aforementioned results with some of the previous reports on optical frequency transfer in the atmosphere. Sprenger *et al.* made a similar rooftop demonstration using a CW diode laser over a 100-m atmospheric link at the ground level [8]. The group achieved an Allan deviation of  $2 \times 10^{-13}$  at 1 s. In addition, a statistics of the beat note frequency measured with a 1-s gate time shows a 70.5-Hz full-width at half-maximum. Compared with this work, the current study reports a frequency instability one

order of magnitude lower at 1 s. Apart from the apparent shorter transmission distance, the smaller frequency fluctuation in this work is likely due to the low-wind condition ( $< 2$  m/s), which means lower index fluctuation due to air turbulence. Such a fact is evident in Fig. 4(b), where continuous frequency measurement over several minutes shows a consistently low frequency fluctuation. More recently, Djerroud *et al.* have reported a coherent optical link across 5 km of turbulent atmosphere based on a CW Nd:YAG laser [9]. A remarkably low Allan deviation of  $1.3 \times 10^{-14}$  is achieved at 1 s, and the stability further improves to  $2 \times 10^{-15}$  at 100 s. The authors, however, did point out that the experiment took place at an observatory 1323 m above the sea level, which could account, at least in part, for the high degree of frequency stability over a long distance. Based on the standard Kolmogorov model of atmospheric turbulence, the power spectral density of refractive index fluctuation  $\Phi_n$  is given by  $\Phi_n(\kappa) = 0.033 C_n^2 \kappa^{-11/3}$ , where  $C_n$  is the index structure constant and  $\kappa$  is the spatial wavenumber. Experimentally, it has been shown that  $C_n$  strongly depends on altitude [20]. For example, the altitude of Huntsville is 200 m, which corresponds to a  $C_n$  of approximately  $10^{-7} \text{ m}^{-1/3}$  for sunny days. At 1323 m, however,  $C_n$  is about  $10^{-8} \text{ m}^{-1/3}$  under similar conditions, which indicates a refractive index fluctuation roughly two orders of magnitude smaller than it at 200 m altitude.

In summary, we have performed what we believe as the first demonstration of atmospheric transfer of optical frequencies using an FL frequency comb. Optical multiheterodyne is used to characterize the excess phase noise due to atmospheric transmission and the relative frequency stability of the transferred spectral lines. The effectiveness of the technique in phase-noise characterization has been analyzed. It has been shown that, for our current transmission distance and heterodyne bandwidth, the group-delay dispersion of air has a negligible effect in the coherent superposition that forms the multiheterodyne signal. This leads to a constructive superposition of the individual beat notes when the pulse overlapping condition is satisfied. With a small, turbulence-induced index fluctuation, the multiheterodyne signal reproduces the zeroth-order phase shift of all the comb lines. When the index fluctuation is large, however, variations in pulse group delay cause distortions of the overall beat note, and the multiheterodyne measurement loses its effectiveness to characterize the behaviors of individual comb lines. Experimentally, we observed a significant comb line broadening after a total propagation distance of 60 m in our open atmospheric link. The phase-noise spectrum indicates large phase modulations at low frequencies, which is believed to be caused by the index fluctuation of the air due to turbulence. Under the low-wind condition, the fractional frequency stability of the transferred spectral lines is measured to be a few parts per  $10^{14}$  at 1-s averaging time. A comparison of this work with previous tests based on CW lasers shows that pulsed lasers can work as well as CW lasers for optical frequency transfer through the atmosphere.

## ACKNOWLEDGMENT

We would like to thank Mr. T. Rogers and Dr. R. Lindquist of the Center for Applied Optics, the University of Alabama in Huntsville, for their assistance in the setup of the atmospheric transmission link.

## REFERENCES

- [1] P. A. Williams, W. C. Swann, and N. R. Newbury, "High-stability transfer of an optical frequency over long fiber-optic links," *J. Opt. Soc. Amer. B*, vol. 25, pp. 1284–1293, 2008.
- [2] M. Musha1, F. Hong, K. Nakagawa, and K. Ueda, "Coherent optical frequency transfer over 50-km physical distance using a 120-km-long installed telecom fiber network," *Opt. Exp.*, vol. 16, pp. 16459–16466, 2008.
- [3] G. Grosche, O. Terra, K. Predehl, R. Holzwarth, B. Lipphardt, F. Vogt, U. Sterr, and H. Schnatz1, "Optical frequency transfer via 146 km fiber link with 10–19 relative accuracy," *Opt. Lett.*, vol. 34, pp. 2270–2272, 2009.
- [4] K. W. Holman, D. J. Jones, D. D. Hudson, and J. Ye, "Precise frequency transfer through a fiber network by use of 1.5- $\mu$ m mode-locked sources," *Opt. Lett.*, vol. 29, pp. 1554–1556, 2004.
- [5] J. Kim, J. A. Cox, J. Chen, and F. X. Kaertner, "Drift-free femtosecond timing synchronization of remote optical and microwave sources," *Nat. Photonics*, vol. 2, pp. 733–736, 2008.
- [6] S. M. Foreman, K. W. Holman, D. D. Hudson, D. J. Jones, and J. Ye, "Remote transfer of ultrastable frequency references via fiber networks," *Rev. Sci. Instrum.*, vol. 78, p. 021101, 2007.
- [7] A. Alatawi, R. P. Gollapalli, and L. Duan, "Radio frequency clock delivery via free-space frequency comb transmission," *Opt. Lett.*, vol. 34, pp. 3346–3348, 2009.
- [8] B. Sprenger, J. Zhang, Z. H. Lu, and L. J. Wang, "Atmospheric transfer of optical and radio frequency clock signals," *Opt. Lett.*, vol. 34, pp. 965–967, 2009.
- [9] K. Djerroud, O. Acef, A. Clairon, P. Lemonde, C. N. Man, E. Samain, and P. Wolf, "Coherent optical link through the turbulent atmosphere," *Opt. Lett.*, vol. 35, pp. 1479–1481, 2010.
- [10] R. P. Gollapalli and L. Duan, "Atmospheric timing transfer using a femto-second frequency comb," *IEEE Photon. J.*, vol. 2, no. 6, pp. 904–910, Dec. 2010.
- [11] I. Coddington, W. C. Swann, and N. R. Newbury, "Coherent multi-heterodyne spectroscopy using stabilized optical frequency combs," *Phys. Rev. Lett.*, vol. 100, p. 013902, 2008.
- [12] S. Kray, F. Spöler, M. Först, and H. Kurz, "Dual femtosecond laser multiheterodyne optical coherence tomography," *Opt. Lett.*, vol. 33, pp. 2092–2094, 2008.
- [13] L. C. Andrews and R. L. Phillips, *Laser Beam Propagation Through Random Media*, 2nd ed. Bellingham, WA: SPIE, 2005.
- [14] N. R. Newbury and W. C. Swann, "Low-noise fiber-laser frequency combs," *J. Opt. Soc. Amer. B*, vol. 24, pp. 1756–1770, 2007.
- [15] G. P. Agrawal, *Nonlinear Fiber Optics*, 3rd ed. New York: Academic, 2001, ch. 2.
- [16] B. Edlén, "The refractive index of air," *Metrologia*, vol. 2, pp. 71–80, 1966.
- [17] R. S. Lawrence and J. W. Strohbehn, "A survey of clear-air propagation effects relevant to optical communications," *Proc. IEEE*, vol. 58, no. 10, pp. 1523–1545, Oct. 1970.
- [18] J. C. Owens, "Optical refractive index of air: Dependence on pressure, temperature and composition," *Appl. Opt.*, vol. 6, pp. 51–58, 1967.
- [19] E. Rubiola and R. Boudot, "Phase noise in RF and microwave amplifiers," in *Proc. IEEE Int. Freq. Control Symp.*, 2010, pp. 109–111 [Online]. Available: <http://arxiv.org/abs/1001.2047>
- [20] A. Ishimaru, *Wave Propagation and Scattering in Random Media*. New York: Academic, 1978, vol. 6, pp. 527–535.

**Ravi P. Gollapalli** (S'09) was born in India. He received the B.Tech. degree in electronics and instrumentation from Nagarjuna University, Guntur, India, in 1998, the M.S. degree in electrical engineering from the University of South Alabama, Mobile, AL, in 2001, and the Ph.D. degree in optical science and engineering from the University of Alabama in Huntsville, Huntsville, AL, in 2011.

Prior to joining the University of Alabama in Huntsville, he was a teaching faculty with Mahatma Gandhi Institute of Technology, Hyderabad, AP, India. He is currently a Postdoctoral Research Associate in the Department of Electrical and Computer Engineering, University of South Alabama, where he has been involved in the modeling and development of algorithms on hyperspectral imagery for the detection of surface and subsurface oil from the 2010 BP Deepwater Horizon oil-spill incident in the Gulf of Mexico.

Dr. Gollapalli is the student member of the Optical Society of America.

**Lingze Duan** (M'01) was born in Beijing, China. He received the B.S. degree in physics from Tsinghua University, Beijing, China, and the Ph.D. degree in electrical engineering from the University of Maryland, College Park, in 1995 and 2002, respectively.

From 2002 to 2004, he was a Postdoctoral Associate in the Research Laboratory of Electronics, MIT, where he studied direct detection of the carrier-envelope phase of femtosecond pulses using semiconductor devices. From 2004 to 2007, he was a Postdoctoral Researcher in the Physics Department, Penn State University, where he developed ultrastable diode laser systems directly stabilized by high- $Q$  optical cavities. In August 2007, he joined the Department of Physics, University of Alabama in Huntsville, Huntsville, AL, as an Assistant Professor. His current research interests include various applications of ultrafast lasers and femtosecond frequency combs as well as the fundamental thermal noise in fiber optic sensors.

Dr. Duan is a member of the Optical Society of America.